Indian Journal of Experimental Biology
Vol. 62, June 2024, pp. 393-399
DOI: 10.56042/ijeb.v62i06.3807

# Synthesis of phycoerythrin-Ag-ZnO nanobiocomposite from marine red algae *Porphyridium purpureum* for anticancer applications against MCF-7 cell line

Baskar G*, Keerthana K, Supriya A, Pravin R, Abinesh AR & Yuvaraaj SA
Department of Biotechnology, St. Joseph's College of Engineering, OMR, Chennai - 600 119, Tamil Nadu, India

*Received 10 July 2023*; *revised 15 March 2024*

The focus on utilization of marine macroalgae for green synthesis of bimetallic nanoparticles with potential applications in cancer treatment has gained a lot of attention in recent years. In this present study, we synthesized a nanobiocomposite using the red pigment R-phycoerythrin from the marine red algae *Porphyridium purpureum* and explored its anticancer potential. This vibrant red fluorescent pigment plays a crucial role as a reducing and stabilizing agent. Ag-ZnO nanobiocomposite was synthesized by green approach using phycoerythrin as a capping agent. The synthesized nanobiocomposite was characterized using UV-Vis spectroscopy, XRD, FT-IR and SEM-EDX techniques. The obtained UV-Vis graph has confirmed the presence of Ag, Zn and phycoerythrin in the synthesized nanobiocomposite. The FT-IR showed the occurrence of Zn–O vibration peak along with hydroxyl and carboxyl groups. The XRD results confirmed the crystalline nature and hexagonal shape of the nanobiocomposite. The overall effect of the synthesized phycoerythrin-Ag-ZnO nanobiocomposite was studied by MTT assay to check its anticancer applications. From the obtained results, the $IC_{50}$ value was found to be 100 µg against MCF-7 cell line. This confirms that the synthesized phycoerythrin-Ag-ZnO nanobiocomposite inhibited the growth of MCF-7 cell line and thus can be efficiently used as a photosensitive drug for chemotherapy in future.

**Keywords:** Bimetallic nanoparticles, Cancer, Chemotherapy, Red seaweed

Chemotherapy plays a crucial part in treating the majority of malignancies but there are still some drawbacks that needs to be addressed. The development of controlled-release technology can overcome those drawbacks of conventional chemotherapy through targeted drug delivery which offers a more effective and safer option[1,2]. Hybrid nanoparticles have made a promising area of research in nanotechnology. By combining different materials, hybrid nanoparticles can have unique properties and functionalities which cannot be achieved through individual particles alone. For instance, bimetallic nanoparticles can offer better control over size, shape and surface properties which can help to improve their efficacy and reduce potential toxicity[3].

Nanoparticles (NPs) are utilized as targeted drug delivery for anti-cancer applications. Metal-based NPs can possess inherent anti-tumor properties such as antioxidant activity[4,5]. The most amazing and promising biological agents are metallic nanoparticles. Silver (Ag) nanoparticles have a wide variety of applications in physical, chemical and biological scientific domains[6]. Additionally, using external energy sources can enhance the anti-cancer properties of NPs. For example, magnetic fields or infrared radiation can be used to induce hyperthermia[7-9]. Due to its antibacterial, antifungal, carcinogenic, antidiabetic, acaricidal, gene delivery, medication delivery and pediculicidal capabilities, ZnO NPs show outstanding potential in biological applications[10,11]. An advantage of employing NPs to treat tumors is the ability to deploy multiple techniques to combat MDR by combining NPs with antitumor medication formulations[12]. Ag nanoparticles can be produced from plants in a cost-effective way without the use of hazardous chemicals, high temperatures or pressure[13,14]. A nanocomposite of Ag-ZnO seems to be particularly suitable for antitumor applications due to its low cost, biocompatibility and low toxicity compared to other noble metals.

Red seaweeds contain R-Phycoerythrin which is 240 kDa oligomeric water-soluble chromoprotein having a 400–650 nm absorption range. Due to its unique spectrum properties, this reddish fluorescent pigment gains interest in biotech applications[15]. The main group of these red algae contains bioactive chemicals such as

*Correspondence:
E-Mail: basg2004@gmail.com

polysaccharides (alginate, agar, and carrageenan), lipids, polyphenols, steroids, glycosides, flavonoids, tannins, saponins, alkaloids, triterpenoids, anthraquinones and cardiac glycosides[16] which is used in the cosmetic, pharmaceutical, food and manure industries. Additionally, it has been observed that phycobiliproteins have therapeutic antioxidant, anti-inflammatory, neuroprotective, anti-cancer and immunomodulatory properties. These bioactive substances act as a capping and reducing agent and also stabilize the synthesized nanoparticle[17,18].

Various substances, including primary and secondary metabolites produced by seaweeds were considered as the interesting sources for biotechnological and industrial uses[19,20]. While phycoerythrin commonly used as a fluorescent targeting probe and food colorant, in the current study, we investigated the role of phycoerythrin as a chemotherapeutic drug when combined with Ag-ZnO nanoparticles. The characterization such as UV-Vis, XRD, FT-IR, SEM-EDX were carried out to study the physiochemical properties of the synthesized nanobiocomposite.

## Materials and Methods

### Chemicals used

The chemicals such as zinc chloride (99% pure), sodium chloride (99% pure), sodium dibasic heptahydrate (99% pure), sodium monobasic monohydrate (99% pure) and sodium nitrate (98% pure) were purchased from LOBA Chemicals, Mumbai, India. All of these chemicals were of analytical grade and used without further purification.

### Collection of *Porphyridium purpureum* biomass

The red seaweed *Porphyridium purpureum* (formerly *P. cruentum*) was collected from Fisheries College and Research Institute, Thoothukudi, Tamil Nadu, India. Epiphytes, extraneous and necrotic materials were removed from *P. purpureum* by washing. Sterilized bottles were used to collect the samples. Samples were properly cleaned using sterile distilled water before being air dried. The moisture from the specimen was drained manually and was later subjected to the sun light to eliminate the moisture for 5 h to get dry biomass. Then the dried biomass was chopped into little pieces and crushed into a fine powder[21].

### Preparation of phosphate buffer for extraction

The extraction of phycoerythrin from *P. purpureum* biomass was carried out using phosphate buffer method. 0.848 g of sodium dibasic heptahydrate ($NaH_2PO_4.7H_2O$) and 5.054 g of sodium monobasic monohydrate ($Na_2HPO_4.H_2O$) were added to 200 mL of distilled water to prepare 20 mM phosphate buffer (pH 7.4).

### Extraction of phycoerythrin pigment from *P. purpureum* biomass

The prepared phosphate buffer and the powdered *P. purpureum* biomass were mixed at a 2:1 ratio in a beaker. A magnetic stirrer was used to agitate the mixture at 200-300 rpm. By this process, the intracellular product phycoerythrin was released from the algal cells and suspended in the prepared buffer solution. The mixture was then centrifuged to remove the biomass at 5000 rpm for 15 min at 4°C. The supernatant was collected for further studies and the pellet containing exopolysaccharides was resuspended in the buffer for further use[22].

### Synthesis of Ag-ZnO nanobiocomposite with phycoerythrin

The 1.698 g of $AgNO_3$ was added to 100 mL of the extract in the beaker. The beaker was subjected stirring using a magnetic stirrer at 80°C for 30 min. Then 0.001 M $ZnCl_2$ solution was added to the extract-$AgNO_3$ mixture at regular intervals[18]. This was added until the zinc precipitates along the bottom and walls of the beaker. The precipitate was then segregated by centrifugation at 10,000 rpm for 10 min. The pellet was retrieved and lyophilized using a freeze dryer at −45°C and 0.150 Kpsi[23].

### Characterization of phycoerythrin-Ag-ZnO nanobiocomposite

A double beam spectrophotometer (Systronics, 2201) was used to analyze the UV-Vis spectroscopy of phycoerythrin-Ag-ZnO nanobiocomposite. The Peaks were observed at wavelengths between 320 and 380 nm. The Functional groups characterization and confirmation of the conjugation of phycoerythrin on the nanobiocomposite was studied by FT-IR analysis using BRUKER RFS 27 MultiRAM system. Powder XRD (Enraf Nonius CAD4-MV31) analysis was done to determine the crystalline nature of the nano-biocomposite. The surface morphology and elemental composition of the synthesized phycoerythrin-Ag-ZnO nanobiocomposite was studied through SEM-EDX analysis.

### Determination of anticancer activity

To cultivate MCF-7 cell lines, 2 mM of glutamine was added to DMEM. 10% FBS was produced at 37ºC using 5% $CO_2$ and 95% air in a humidified incubator. After two days, the media was switched back to a fresh culture medium (DMEM with 10%

FBS) and the growth of multinucleation in the cells was used to assess the level of differentiation. Cells were planted in 96-well tissue culture plates with $5\times10^3$ cells in 100 µL medium per well. The MCF-7 cells were exposed to different amounts of lyophilized material (100 ng, 10 ng, 1 ng, and 1 µg). After being cultured for 24 hr, cells were treated with MTT reagent and left undisturbed for an additional 4 hr. The reaction was halted by aspirating the media, dissolving the formazan crystals that have formed in DMSO and analyzing the absorbance at 570 nm which is directly proportional to cell viability. Using Eq. 1, the percentage of cytotoxicity was calculated. The graph was plotted and the $IC_{50}$ value was determined using these values.

$$\text{Percentage of cytotoxicity, \%} = \frac{1-OD\ control-\ OD\ test)}{OD\ control} * 100 \quad \dots (1)$$

## Results and Discussion

### UV-Vis spectral analysis of synthesized phycoerythrin-Ag-ZnO nanobiocomposite

UV-Vis spectral analysis was conducted on the synthesized phycoerythrin-Ag-ZnO nanobiocomposite which revealed distinctive peaks within the wavelength range of 320 to 800 nm. The obtained spectral graph was depicted in Fig. 1. The identification of specific peaks provided evidence for the elemental composition of the synthesized nanobiocomposite. Notably, the presence of Zn was verified by the detection of a peak in the range of 320-350 nm. While the presence of Ag was indicated by a peak at 400 nm. Furthermore, the characteristic peak at 500 nm confirms the presence of phycoerythrin within the nanobiocomposite. The UV-visible analysis affirmed the coexistence of phycoerythrin, Ag and ZnO in the synthesized phycoerythrin-Ag-ZnO nanobiocomposite.

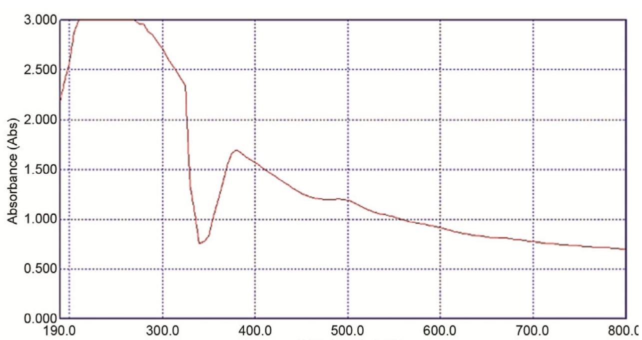


Fig. 1 — UV-Vis spectrum of the synthesized phycoerythrin-Ag-ZnO nanobiocomposite

### FT-IR analysis of synthesized phycoerythrin-Ag-ZnO nano-biocomposite

The presence of functional groups within the synthesized phycoerythrin-Ag-ZnO nanobiocomposite was characterized through FT-IR analysis. The peaks were observed between 500 and 3500 $cm^{-1}$. The observed peaks were shown in Fig. 2. The peak observed at 599.31 $cm^{-1}$ confirms the presence of Zn-O stretching in the nanobiocomposite. A medium N-H bending was identified by the peak at 1648.23 $cm^{-1}$, while the O-H stretching at 3274.44 $cm^{-1}$ affirmed the existence of Ag metal in the nanobiocomposite. The peak at 859.76 $cm^{-1}$ shows the presence of medium C=C bending and the occurrence of strong C=C bending of the alkene generated the absorption peak at 996.13 $cm^{-1}$. The significant absorption peak at 1068.99 $cm^{-1}$ was attributed to C-O stretching, while the peak at 1234.82 $cm^{-1}$ was indicative of moderate C-N stretching. The absorption peak at 3274.44 $cm^{-1}$ was attributed to the -OH stretching of the -COOH group.

The presence of these functional groups particularly those associated with phycoerythrin protein, implicated in the capping of Ag-ZnO nanobiocomposite was confirmed[24,25]. The FT-IR spectroscopic study suggests that the secondary structure of proteins in *P. purpureum* remains unaffected by their interaction with $Ag^{+}$ ions or nanoparticles[26,27].

### SEM- EDX analysis of synthesized phycoerythrin-Ag-ZnO nanobiocomposite

SEM analysis helps in studying the surface's shape, structure and distribution of NPs and also offers information about nanoscale particles. Information about the metals present within the material can be checked by EDAX or EDS analysis[28-30]. The surface morphology of the phycoerythrin-Ag-ZnO nano-biocomposite was studied through observed SEM

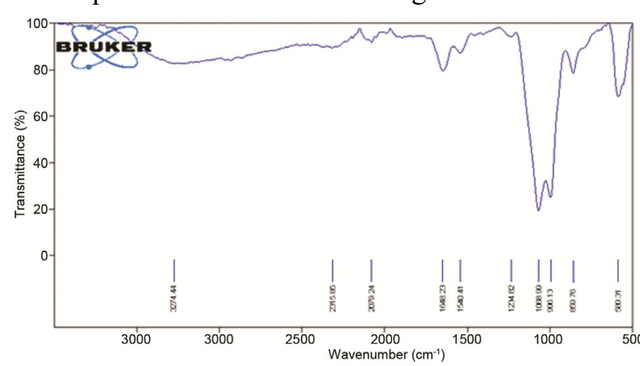


Fig. 2 — FT-IR spectrum of the synthesized phycoerythrin-Ag-ZnO nanobiocomposite

images shown in Fig. 3 under the resolution of 1 and 2 µm. The elemental distribution of Zn, Ag and O in phycoerythrin-Ag-ZnO nanobiocomposite was observed from EDX images shown in Fig. 4. The presence of Zn was confirmed by the peak at 1 keV in the EDX analysis while the presence of Ag was confirmed by the peak between 2.5 and 3 keV. The results obtained from EDX analysis was shown in Fig. 5. The peak corresponding to oxygen in EDX spectrum might be due to the presence of phycoerythrin protein in the nanobiocomposite[31,32].

**XRD analysis of synthesized phycoerythrin-Ag-ZnO nanobiocomposite**

The crystalline nature of the synthesized *phycoerythrin-Ag-ZnO* nanobiocomposite was studied with peaks observed from the XRD data. Various peaks observed at 2 theta angles of 27.45, 31.83, 45.51, 56.51 and 66.30 were shown in Fig. 6. The hexagonal wurtzite ZnO along with face-centered-cubic (fcc) metallic Ag was verified using (JCPDS file no. 36-1451) and (JCPDS file no. 04-0783). The average size of synthesized *phycoerythrin-Ag-ZnO* nanobiocomposite was calculated with Debye – Scherer's formula,

$$D = k\,\lambda / \beta \cos\theta,$$

where $\lambda$ - X-ray wavelength, $\beta$ - full width at half maximum of the XRD peak, and $\theta$ is the Bragg angle. The average size of synthesized *phycoerythrin-Ag-ZnO* nanobiocomposite was found to be 32.97 nm[33-35].

**Anticancer activity of synthesized phycoerythrin-Ag-ZnO nanobiocomposite**

The anticancer activity of the synthesized phycoerythrin-Ag-ZnO nanobiocomposite against

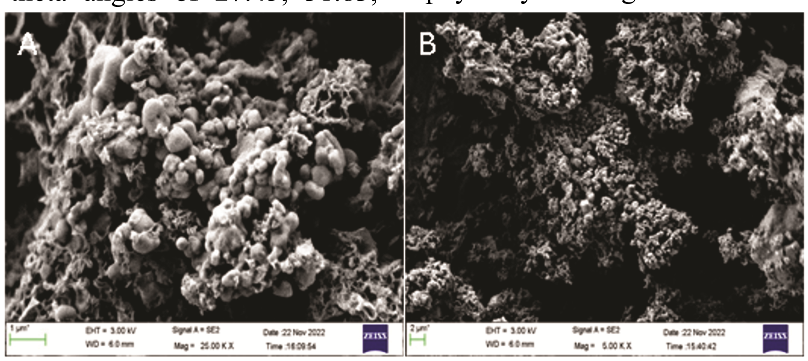


Fig. 3 — (A & B) SEM images of phycoerythrin-Ag-ZnO nanobiocomposite under the resolution of 1 and 2 µm, respectively

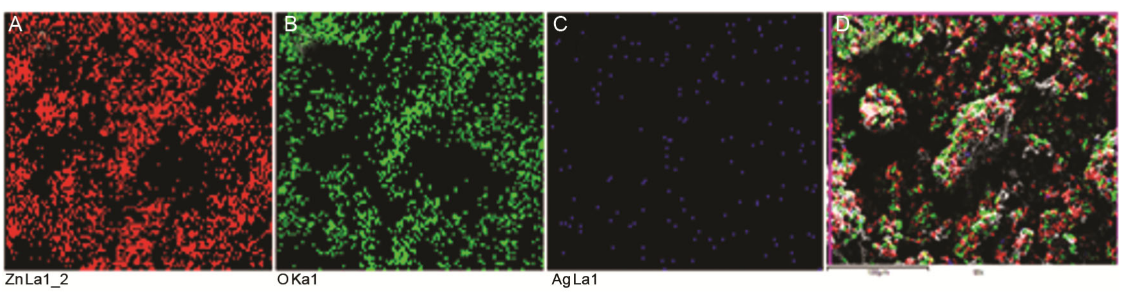


Fig. 4 — Elemental distribution of Zn, Ag, and O in phycoerythrin-Ag-ZnO nanobiocomposite (A) Zn distribution; (B) O distribution; (C) Ag distribution; and (D) overall distribution of Zn, Ag and O

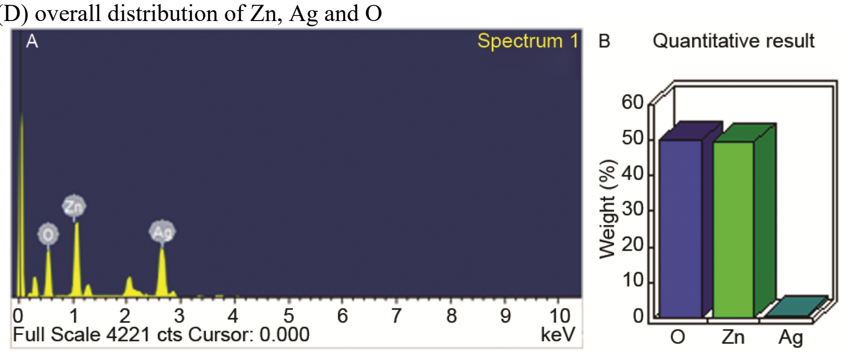


Fig. 5 — (A) EDX spectrum; and (B) Composition distribution of the synthesized phycoerythrin-Ag-ZnO nanobiocomposite

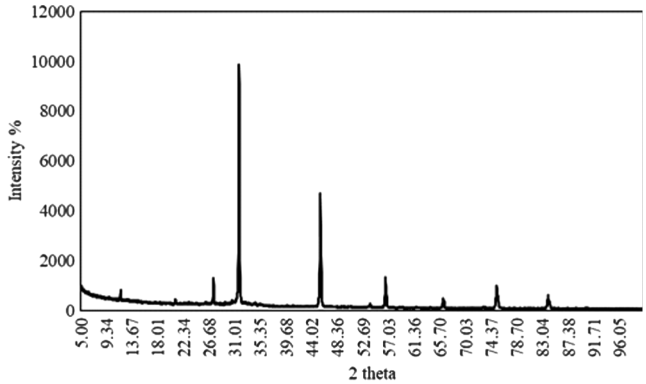


Fig. 6 — XRD analysis of the synthesized phycoerythrin-Ag-ZnO nanobiocomposite

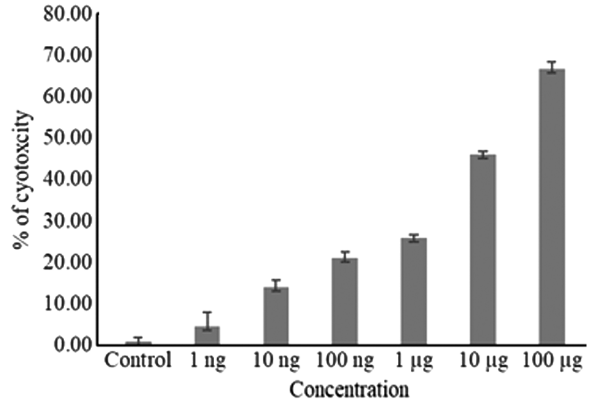


Fig. 7 — Anticancer activity of synthesized phycoerythrin-Ag-ZnO nanobiocomposite against MCF-7 cell line

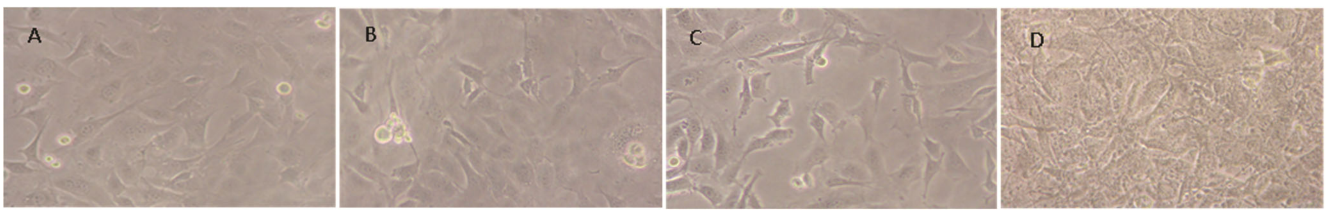


Fig. 8 — Microscopic images of anti-cancer activity of phycoerythrin-Ag-ZnO nanobiocomposite against MCF-7 cell line under various concentrations (A) control; (B) 1 ng; (C & D) 1 and 100 µg

breast cancer cell line (MCF-7) was studied through MTT assay. The cell line was subjected to various concentrations (1 ng, 10 ng, 100 ng, 1 µg, 10 µg, and 100 µg) of the nanobiocomposite. The cytotoxicity was observed and contrasted with the cell control. Using the obtained optical values, the percentage of cytotoxicity was estimated. From the observed results, it was noted that cell line survival decreased with an increase in nanocomposite concentration which depicts that the synthesized phycoerythrin-Ag-ZnO nanobiocomposite exhibits anticancer drug properties. The obtained results have been depicted in Figs 7 and 8. The lowest concentration of 1 ng showed cell cytotoxicity of 9%, while 100 µg concentration showed the maximum cytotoxicity of 59%. The $IC_{50}$ value indicates that 50% of cell death occurs at 100µg concentration of the synthesized phycoerythrin-Ag-ZnO nanobiocomposite. The phycoerythrin-Ag-ZnO nanobiocomposite was found to be efficient when compared to starch-based copper nanoparticles, selenium nanoparticles and nickel nanoparticles[36-38]. Thus, the synthesized nanobiocomposite carrying phycoerythrin was observed to be effective, reliable and a potential anti-cancer drug making it useful in the biomedical field. The synthesized phycoerythrin-Ag-ZnO nanobiocomposite can also be utilized for medication administration which lowers the harmful effect and enhances the drug availability[39-41].

## Conclusion

The phycoerythrin pigment with its recognized potential as a chemotherapeutic drug was successfully extracted and purified from the marine algae *Porphyridium purpureum*. Subsequently, this valuable pigment was used to synthesize phyco-erythrin-Ag-ZnO nanobiocomposite. Evaluating its therapeutic potential, the phycoerythrin-Ag-ZnO nanobiocomposite demonstrated notable anti-cancer activity against the MCF-7 cell line with an $IC_{50}$ value of 100 µg. The finding underscores its efficacy in inducing apoptosis and significantly reducing MCF-7 cell viability. Beyond its anticancer properties, the phycoerythrin-Ag-ZnO nanobiocomposite holds promise for diverse applications in drug delivery. This innovative approach not only expands the understanding of phycoerythrin's potential but also opens avenues for multifaceted applications in the burgeoning field of nanomedicine. Overall, this study reveals that the synthesized nanobiocomposite exhibits promising attributes as a cost-effective, eco-friendly and efficient chemotherapeutic agent as evidenced by its successful performance against the MCF-7 cell line. This makes the synthesized phycoerythrin-Ag-ZnO nanobiocomposite as a valuable contribution to the field of cancer therapy and positions it as a versatile platform for further exploration in nanomedicine applications.

## Conflict of interest

Authors declare no competing interests.

## References


1 Gavas S, Quazi S & Karpiński TM, Nanoparticles for Cancer Therapy: Current Progress and Challenges. *Nanoscale Res Lett*, 16 (2021) 173.

2 Rajendran R & Mani A, Photocatalytic, antibacterial and anticancer activity of silver-doped zinc oxide nanoparticles. *J Saudi Chem Soc*, 24 (2020) 1010.

3 Eshaghzadeh H, Shahbazi M, Akhavan SR & Pereira L, Purification and characterization of phycoerythrin from the Caspian Sea red macroalga (Osmundea caspica). *J Appl Phycol*, 35 (2022) 317.

4 Yu J, Liu S, Wang Y, He X, Zhang Q, Qi Y, Zhou D, Xie Z, Li X & Huang Y, Synergistic enhancement of immunological responses triggered by hyperthermia sensitive Pt NPs via NIR laser to inhibit cancer relapse and metastasis. *Bioact Mater*, 7 (2022) 389.

5 Baran MF, Keskin C, Baran A, Hatipoğlu A, Yıldıztekin M, Küçükaydın S, Kurt K, Hoşgören H, Sarker MMR, Sufianov A, Beylerli O, Khalilov R & Eftekhari A, Green Synthesis of Silver Nanoparticles from *Allium cepa L.* Peel Extract, Their Antioxidant, Antipathogenic, and Anticholinesterase Activity. *Molecules*, 28 (2023) 2310.

6 Bloch K, Pardesi K, Satriano C & Ghosh S, Bacteriogenic platinum nanoparticles for application in nanomedicine. *Front Chem*, 9 (2021) 624344.

7 Alizade A & Terzi MY, *In vitro* apoptotic and anti-proliferative effects of propranolol on human breast cancer cells. *Indian J Exp Biol*, 62 (2024) 326.

8 Nugraha AS, Han M, Ashok A, Kang Y, Kim J, Alshehri SM, Ahamad T, Bandô Y & Yamauchi Y, Synergistic mesoporous bimetallic gold-silver nanoparticles: Synthesis, structure, and superior electrocatalytic activity. *Nano Energy*, 116 (2023) 108770.

9 Bisht G & Rayamajhi S, ZnO nanoparticles: a promising anticancer agent. *Nanobiomedicine*, 3 (2016) 9.

10 Jeong GH, Bak D, Lee H, Cho JY, Kang SH, Chung BY, Park S & Bai H, Anti-cancer effects of plant-derived *Micromonospora sp.* M2 against A549 and MCF-7 cell lines. *Biosci Biotechnol Biochem*, 2024 (2024).

11 Abed A, Derakhshan M, Karimi M, Shirazinia M, Mahjoubin-Tehran M, Homayonfal M, Hamblin MR, Mirzaei SA, Soleimanpour H, Dehghani S & Dehkordi FF, Platinum nanoparticles in biomedicine: preparation, anti-cancer activity, and drug delivery vehicles. *Front Pharmacol*, 13 (2022) 797804.

12 Ganesan AR, Kannan M, Rajan DK, Pillay A, Shanmugam M, Sathishkumar P, Johansen JG & Tiwari BK, Phycoerythrin: a pink pigment from red sources (rhodophyta) for a greener biorefining approach to food applications. *Crit Rev Food Sci Nutr*, 63 (2022) 10928.

13 Yamamoto S, Yamamoto S & Tokuda M, Optimal nitrogen source for the recovery of phycoerythrin in discolored *Rhodomonas sp. Algal Res*, 80 (2024) 103521.

14 Aziz E, Batool R, Khan MU, Rauf A, Akhtar W, Heydari M, Rehman S, Shahzad T, Malik A, Mosavat SH & Plygun S, An overview on red algae bioactive compounds and their pharmaceutical applications. *J Complement Integr Med*, 17 (2020).

15 Sonani RR, Rastogi RP, Patel R & Madamwar D, Recent advances in production, purification and applications of phycobiliproteins. *World J Biol Chem*, 7 (2016) 100.

16 Sudhakar M, Dharani G & Paramasivam A, Evaluation of antimicrobial, antioxidant and cytotoxicity potential of R-phycoerythrin extracted from *Gracilaria corticata* seaweed. *Curr Res Green Sustain Chem*, 6 (2023) 100352.

17 Javed MR, Shafiq S, Allah EFA, Salman M, Perver N, Anwar A & Zahra FT, Cyanobacteria-Based green synthesis of nanoparticles for industrial applications. In: Pharmaceutical and Nutraceutical Potential of Cyanobacteria, (Eds. Mehmood MA, Verma P, Shah MP, Betenbaugh MJ; Springer, Cham.), 2024, 195.

18 Baskar G & Supria Sree NS, Anticancer activity of gelatin-asparaginase nanobiocomposite against cervical and brain cancer cell lines. *J Drug Deliv Sci Technol*, 57 (2020) 101689.

19 El-Beltagi HS, Mohamed AA, Mohamed HI, Ramadan KMA, Barqawi AA & Mansour AT, Phytochemical and potential properties of seaweeds and their recent applications: A Review. *Mar Drugs*, 20 (2022) 342. doi: 10.3390/md20060342.

20 Ahmed A, Usman M, Ji Z, Rafiq M, Yu B, Shen Y & Cong H, Nature-inspired biogenic synthesis of silver nanoparticles for antibacterial applications. *Mater Today Chem*, 27 (2023) 101339.

21 Lauceri R, Chini Zittelli GC & Torzillo G, A simple method for rapid purification of phycobiliproteins from *Arthrospira platensis* and *Porphyridium cruentum* biomass. *Algal Res*, 44 (2019) 101685.

22 Sheena T, Jyothish B & Jacob J, Preparation, characterization, and in vitro evaluation of the anticancer activity of Ce3+ doped CuFe2O4 spinel nanoparticles in MCF-7 cell lines. *Chemical Physics Impact*, 8 (2024) 100423.

23 Xu Y, Hou Y, Wang Y, Wang Y, Li T, Song C, Wei N & Wang Q, Sensitive and selective detection of Cu2+ ions based on fluorescent Ag nanoparticles synthesized by R-phycoerythrin from marine algae *Porphyra yezoensis. Ecotoxicol Environ Saf*, 168 (2019) 356.

24 Sagar V, Patel RR, Singh S & Singh M, Green synthesis of silver nanoparticles: methods, biological applications, delivery and toxicity. *Mater Adv*, 4 (2023) 1831.

25 Ravi A & Gurunathan B, Acrylamide mitigation in fried kochchi kesel chips using free and immobilized fungal asparaginase. *Food Technol Biotechnol*, 56 (2018) 51.

26 Veeramani C, Newehy ASE, Aloud AA, Alsaif MA & Al-Numair KS, Nutritional plants, phytochemicals, microorganisms-derived silver nanoparticles and their diabetic managements. In: *Silver Nanoparticles for Drug Delivery*. (Ed. Kesharwani P; Academic Press, Elsevier Inc.), 2023, pp. 241-264. DOI:10.1016/B978-0-443-15343-3.00014-0.

27 Wasilewska A, Klekotka U, Zambrzycka M, Zambrowski G, Święcicka I & Kalska-Szostko B, Physico-chemical properties and antimicrobial activity of silver nanoparticles fabricated by green synthesis. *Food Chem*, 400 (2023) 133960.

28 Shaikh SM & Desai P, Magnesium oxide nanoparticles administered orally promote degenerative changes and dysfunctioning in the brain. *Indian J Exp Biol*, 62 (2024) 229.

29 Shet VB, Kumar PS, Vinayagam R, Selvaraj R, Vibha C, Rao SV, Pawan SM, Poorvika G, Quintero VM, Ujwal P, Rajesh KS, Dubey A & Yumnam S, Cocoa pod shell mediated silver nanoparticles synthesis, characterization, and their application as nanocatalyst and antifungal agent. *Appl Nanosci*, 13 (2023) 4235.

30 Abboud Y, Saffaj T, Chagraoui A, El Bouari A, Brouzi K, Tanane O & Ihssane B, characterization and antimicrobial activity of copper oxide nanoparticles (CONPs) produced using brown alga extract (*Bifurcaria bifurcata*). *Appl Nanosci*, 4 (2017) 571.
31 Castro-Varela P, Rubilar M, Martínez-Férez A, Fuentes-Ríos D, López-Romero JM, Alarcón C, Abdala-Díaz R & Figueroa FL, R-phycoerythrin alginate/shellac beads by external gelation: Process optimization and the effects of gastrointestinal digestion for nutraceutical applications. *Algal Res*, (2024) 103473.
32 Wang L, Xi Q, Song Y, Wang X, Gu W, Niu J, Sun Y, Srinuanpan S & Wang G, Green synthesis of gold nanoparticles by phycoerythrin extracted from *Solieria tenuis* as an efficient catalyst for 4-nitrophenol reduction and degradation of dyes in wastewater. *Mater Today Sustain*, 23 (2023) 100435.
33 Korak T, Emrence Z, Ekmekci SS, Abaci N & Ergül E, Effect of Nigella sativa L. extract and thymoquinone on the genes responsible for cell proliferation, migration and NK cell cytotoxicity in breast cancer. *Indian J Exp Biol*, 62 (2024) 317.
34 Bekasova OD, Properties and potential applications of bioconjugates of R-phycoerythrin with Ag or CdS nanoparticle synthesized in its tunnel cavity: A review. International Journal of Biological *Macromolecules*, 255 (2024) 128181.
35 Hasanin M, Al Abboud MA, Alawlaqi MM, Abdelghany TM & Hashem AH, Ecofriendly synthesis of biosynthesized copper nanoparticles with starch-based nanocomposite: antimicrobial, antioxidant, and anticancer activities. *Biol Trace Elem Res*, 1 (2021) 14.
36 Boonyuen S, Paramasivam S, Rajan R, Phromsatit T, Teerawatananond T, Tantayanon S, Arpornmaeklong P & Shirosaki Y, Exploring copper (II) porphyrin complexes and their derivatives for electrochemical analysis and biological assessment in the study of breast cancer (MCF-7) cell lines. *Environ Res*, 250 (2024) 118489.
37 Packirisamy V, Ayyadurai B, Perumal D, Pandurangan P, Ranishree JK, Dhandapani P & Nallamuthu T, Green synthesis of R-phycoerythrin protected gold nanoclusters for sensitive detection of mercury(II) ions and their antibacterial properties. *J Mater Res*, 38 (2023) 3009.
38 Hashem AH, Selim TA, Alruhaili MH, Selim S, Alkhalifah DHM, Al Jaouni SK & Salem SS, unveiling antimicrobial and insecticidal activities of biosynthesized selenium nanoparticles using prickly pear peel waste. *J Funct Biomater*, 13 (2022) 112.
39 Hashem AH, Al Abboud MA, Alawlaqi MM, Abdelghany TM & Hasanin M, Synthesis of nanocapsules based on biosynthesized nickel nanoparticles and potato starch: antimicrobial, antioxidant, and anticancer activity. *Starch Stärke*, 74 (2022) 2100165.
40 Baskar G & Supria Sree NS, Synthesis, characterization and anticancer activity of β-cyclodextrin-asparaginase nano biocomposite on prostate and lymphoma cancer cells. *J Drug Deliv Sci Technol*, 55 (2020) 101417.
41 Baskar G, Abinesh AR, Sheik Mohammed Raja A, Keerthana K, Supriya A & Pravin R, Green synthesis, characterization and anticancer activity of fungal asparaginase from Aspergillus terreus conjugated on MgO-ZnO nanocomposite against liver cancer cells. *Indian J Exp Biol*, 61 (2023) 761.